Catalysis
Science &
Technology

Accepted Manuscript

ROYAL SOCIETY
OF CHEMISTRY

www.rsc.org/catalysis

Selective catalytic reduction of NO by NH_3 over CuO-CeO_2 in the presence of SO_2

Bo Li[a], Zhiyuan Ren[b], Zhaoxia Ma[a], Xiaodong Huang[a], Fu Liu[a], Xiaobin Zhang[a], Hangsheng Yang[a*]

[a] *State Key Laboratory of Silicon Materials, School of Materials Science and Engineering, Zhejiang University, Zheda Road 38, Hangzhou 310027, China*

[b] *Foreign Economic Cooperation Office, Ministry of Environmental Protection, China, HouyingfangHutong 5, Xicheng District, Beijing 100035, China*

---

[*] To whom correspondence should be addressed. Tel/Fax: +86-571-87951404;

E-mail: hsyang@zju.edu.cn

Abstract:

SO_2 induced deactivation of selective catalytic reduction of NO over CuO-CeO_2 was studied. In the case of reaction under low O_2 concentration of 1.0 vol%, SO_2 severely deactivated the catalyst at 240 °C with a surface S atomic concentration as low as 1.34 %. However, the deactivated catalyst could be reactivated during online NO reduction under 5.0 vol% O_2 without decreasing the surface S concentration of catalyst, which could be attributed to the involvement of NO_2 into the reactions. NO_2 could promote the NO removal through three reaction routes: fast SCR reaction; reaction between NO_2 and NH_3, and reaction between NO_2 and NH_4^+. Especially under conditions of 10% O_2, the reaction between NO_2 and NH_3/NH_4^+ induced the formation of extra $NH_{X<3}$ species which promoted the decomposition of surface deposited sulfate to SO_2 with the assistance of Ce_2O_3, thus suppressed the accumulation of sulfate on the catalyst surface, and finally suppressed the SO_2 induced catalyst deactivation.

Keywords: Selective catalytic reduction; NO_X; SO_2 deactivation; CeO_2; sulfate decomposition

1. Introduction

Nitrogen oxides (NO_X) are the main reason for the formation of acid rain and photochemical smog, which are harmful for the ecosystem and humanity. Selective catalytic reduction (SCR) is the dominant technology to control the NO_X emission from stationary sources including power boilers and combustion furnaces [1, 2]. Traditional V_2O_5-WO_3/TiO_2 catalysts have been widely employed at high temperature but with several defects, such as high toxicity of active components, high activity for SO_2 oxidation, and formation of N_2O at high temperature [3-5], which stimulated the continuing efforts to develop high performance catalysts. Among them, the development of low temperature active catalysts, which could be installed after the dust removal facility, is highly desired. MnO_X, CuO_X, CeO_X and their composites are typically studied transition metal oxides as promising low temperature SCR catalysts [6-12]. Especially, ceria is found to promote NO removal via the redox cycle between Ce^{4+} and Ce^{3+} [10, 13-15], and Cu^{2+} species in the CeO_2 matrix is more catalytically active than Cu^{2+} in the CuO matrix [12, 16], and the synergistic effect between Cu and Ce species was also reported to improve the oxygen activation and NO_X adsorption over Cu-CeO_X and CuO-CeO_2-TiO_2 catalysts [17-19].

Flue gases always contain small concentrations of SO_2 even after desulphurization. The SO_2 induced catalyst deactivation is still the main barrier for the application of low temperature active SCR systems [6, 8, 20-23]. In fact, the influences of SO_2 on the NO removal over low temperature SCR catalysts have been studied extensively, and it is well accepted that the catalyst deactivation was mainly due to the deposition of ammonia sulfate/sulfites which covered the active sites of the catalyst at low temperature [22]. Recent results found that the fast SCR reaction involved NO_2 was less affected by SO_2 deactivation than the standard SCR [24], and the presence of large amounts of NO could destabilize the ammonium nitrates and decomposed them at lower temperatures [25]. Also, oxygen in the NO-containing stream was found to play an important role in the NO conversion and selectivity of the SCR reaction, which promote the formation of NO_2 and accelerate of the SCR reaction [26-29]. Moreover, the addition of CeO_2 into the catalysts was also reported to play in important role for the promotion of resistance to SO_2 induced catalyst deactivation [11, 30]. However, further studies are still expected to pursue the possibility for the de-NO_X at low temperature in the presence of SO_2.

In this study, we found that the SO_2 induced catalyst deactivation could be suppressed at relatively low temperature of 240 °C via the reaction between NH_3 (NH_4^+) and NO_2 (oxidized from NO). Moreover, this reaction also induced the formation of $NH_{X<3}$ species which promoted the decomposition of sulfate to SO_2 with the assistance of Ce_2O_3, thus suppressed the accumulation of ammonia sulfate on the catalyst surface.

2. Experimental

Traditional precipitation was applied to prepare the catalyst. Typically 6.0 mmol of cetyltrimethylammonium bromide was dissolved in 300 ml distilled water at ambient temperature, then 85 mmol of $Cu(NO_3)_2$ and 15 mmol of $Ce(NO_3)_3$ were added into the above solution under magnetic stirring. After 30 min of continue stirring, ammonium hydroxide was gradually added until the pH value of the mixed solution reached to 10, and the suspended solution was aged at 90 °C for 3 h. Finally, the precipitate was filtered, washed with distilled water, dried in the oven at 100°C over night, and then milled and calcined at 300 °C for 5 h for later use.

X-ray photoelectron spectroscopy (XPS) data were obtained using a Thermo ESCALAB 250. The X-ray source was an Al Kα radiation. All binding energies were referenced to a 284.8 eV C1s. The used TG analyzer was NETZSCH STA 449F3 and the heating rate was 10 °C/min.

NH_3-temperature-programmed desorption (NH_3-TPD) experiments were performed using 100 mg of each catalyst to determine their NH_3 adsorption ability. The sample was pretreated in a helium stream (30 ml/min) at 500 °C for 1 h, and then cooled to 60 °C. The pretreated sample was exposed to a mixed flow of 10% NH_3 in argon at a flow rate of 20 ml/min for 2 h at ambient temperature, and then heated from 100 °C to 800 °C at a heating rate of 10 °C/min. The NH_3-TPD data was recorded on-line by a mass-quadrupole detector (QIC 20).

FTIR experiments were performed on CuO-CeO_2 catalyst recorded with a Nicolet 5700 Fourier Transform spectrometer (0.09 cm^{-1} resolution). CuO-CeO_2 catalyst after each treatment was cooled to room temperature and then purged by N_2 for 1 hour. Then the powder samples were compressed in KBr-supporting disks to obtain the IR spectra.

SCR activity measurements and NO oxidation experiments were performed as previous studies using 0.2 g catalyst pasted on three Al plates (4cm × 10 cm) [6-8]. The inlet and outlet concentrations of NO, NO_2, SO_2, and O_2 were monitored by Testo AG testo 340.

Catalysts were deactivated/regenerated by 550 ppm NO, 550 ppm NH_3, 200 ppm SO_2 when used under 150,000 h^{-1} GHSV at 240 °C with different O_2 concentration. The SO_2 deactivated samples were expressed as $SD_{[C]}(T)$, where T stood for the time (minute) on stream and [C] stood for the O_2 concentration.

3. Results and discussion

3.1 Impacts of O_2 and SO_2 on Catalytic activity

NO conversion was significantly affected by oxygen concentration and temperature as shown in Fig. 1. The NO conversion increased from 32.2% to 40% and 45.2% with the increasing of oxygen concentration from 1.0 vol% to 5.0 vol% and 10.0 vol% at 160 °C, respectively. NO conversion was further promoted by temperature increasing and reached 53%, 65.6%, and 69.4% with 1.0 vol%, 5.0 vol% and 10.0 vol% of O_2 at 220 °C, respectively. For temperature at 240 °C or above, the NO conversion was reduced under O_2 concentration above 5% due to the side reaction of NH_3 over oxidation [6-8].

The O_2 concentration significantly affects SO_2 deactivation and regeneration behavior over $CuO-CeO_2$ catalyst as shown in Fig. 2. For a fresh catalyst with 57.3%

NO conversion at 240 °C (section A) under 1.0 vol% O_2, the NO conversion decreased sharply to 8.7% within 1.5 h with 200 ppm SO_2 (section B). After the catalyst was regenerated during online SCR for 2 h with 5.0 vol% O_2 (section C), the NO conversion recovered and reached 61.8%, however, SO_2 still deactivated the catalyst slightly and the NO conversion decreased to 50.9% in 1.5 h (section D). When the catalyst was worked again in 10.0 vol% O_2 (section E), the NO conversion recovered to 60.2% again, and SO_2 deactivation could be minimized (black line shown in section F). In summary, SO_2 deactivation is O_2 concentration dependent and high O_2 concentration can not only recover the deactivated catalyst, but also minimize SO_2 deactivation at relatively low temperature of 240 °C.

3.2 NO oxidation

The oxidation of NO to NO_2 was studied as shown in Fig. 3. Signal of NO_2 was not detected at 100-300 °C with 1.0 vol% oxygen. Once the oxygen concentration increased to 5.0 vol%, NO_2 was first detected at 160 °C and reached 180 ppm at 300 °C. Under 10.0 vol% O_2, 260 ppm NO_2 was detected at 300 °C. All the results demonstrated that the catalytic oxidation of NO to NO_2 was O_2 concentration depended on O_2 concentration, which should be able to accelerate the SCR reaction especially at low temperatures [29, 31]. From Fig. 3, sufficient NO_2 was produced at 240 °C under O_2 concentration above 5.0 vol%.

3.3 NH_3-TPD and NH_3-TPO

The NH_3-TPD technique was employed to determine the acidic sites in the catalyst and its NH_3 adsorption behavior. As shown in Fig. 4a, the NH_3 desorption started at 100 °C and reached the maximum desorption at 215 °C and then decreased with further increasing the temperature, almost no NH_3 was desorbed at temperature above 300 °C. Evidently, NH_3 was adsorbed on the surface of CuO-CeO_2 during SCR of NO at 240 °C.

Fig. 4b shows the influence of O_2 on NH_3 oxidation. NH_3 oxidation started at 150 °C (9.7%) and enhanced with temperature and reached 41% at 300 °C under 1 vol% O_2, indicating that NH_3 could be oxidized with a relative low O_2 concentration of 1 vol%. NH_3 oxidation, which was further promoted by high O_2 concentration, reached a conversion of 95.5% and 97.8% at 300 °C with 5 vol% and 10 vol% O_2, respectively. Fig. 4b also shows the influence of O_2 concentration on NO and NO_2 selectivities from NH_3 oxidation. NO and NO_2 were not detected under 1 vol% O_2 at 100-300 °C. Under 5 vol% O_2, NO was detected above 200 °C and reached 132 ppm at 300 °C with a NO selectivity of 24%, but NO_2 was not detected throughout the experiments. When the O_2 concentration increased to 10 vol%, not only NO was detected at 160 °C and reached 90 ppm at 300 °C, but NO_2 was also detected above 240 °C and reached 43 ppm at 300 °C, the selectivity of NO and NO_2 was 16.3% and 7.8%, respectively. In summary, a relatively low concentration of O_2 is sufficient to promote NH_3 activation, and high O_2 concentration promoted the over oxidation of NH_3 to NO (even NO_2), especially at temperature above 240 °C.

3.4 XPS analysis

Fig. 5 shows the XPS spectra of fresh and used CuO-CeO$_2$. The O 1s bands of the samples were shown in Fig. 5a, the binding energy at about 529.6 eV corresponded to the lattice oxygen (denoted as O$_\beta$), and the band at about 531.6 eV corresponded to the surface adsorbed oxygen (-OH) (denoted as O$_\alpha$) [32], and the ratio of O$_\alpha$/(O$_\alpha$+O$_\beta$) over fresh CuO-CeO$_2$ was 45.9%. The lattice oxygen appeared as the adsorption sites for SO$_2$ and the adsorbed oxygen played an important role in the formation of sulfites/sulfates [33]. The ratio of O$_\alpha$/(O$_\alpha$+O$_\beta$) increased to 60.9% and 76.3% over SD$_{[5\%]}$(300) and SD$_{[10\%]}$(540) after oxygen concentration increased during SO$_2$ deactivation in Fig. 2. The increase of adsorbed oxygen suggested the deposition of sulfates [6, 8] and the strong adsorption of NO$_2$ as shown in Fig. 7.

The complex spectrum of Ce 3d was deconvoluted into eight components in Fig. 5b, and those peaks detected at 882.8, 889.2, 898.7, 901.1, 908.2, and 917.6 eV represent the 3d^{10}4f^0 initial electronic state corresponding to Ce^{4+} species [34]. And the peaks at 885.1 eV and 903.5 eV arise from Ce^{3+} species [35]. The results indicated that CeO$_2$ and Ce$_2$O$_3$ are both existed in CuO-CeO$_2$. The ratio of Ce^{3+}/(Ce^{3+} + Ce^{4+}) is calculated to be 21.7%, 16%, 9.9%, and 9.4% over fresh catalyst, SD$_{[1\%]}$(90), SD$_{[5\%]}$(300), and SD$_{[10\%]}$(540) respectively, which demonstrated that part of Ce^{3+} was oxidized to Ce^{4+} when O$_2$ and SO$_2$ concentrations were increased.

From the Cu 2p bands of the samples shown in Fig. 5c, the binding energy at 954 eV and 934 eV corresponded well with Cu^{2+} over fresh catalyst, SD$_{[1\%]}$(90),

$SD_{[5\%]}(300)$, and $SD_{[10\%]}(540)$ [36], which indicated that the sulfation of the catalyst did not change the chemical state of Cu^{2+}. According to our previous results, Cu^{2+} is the main active component at low temperatures [6-8], Cu^{2+} ions were ready to be reduced to Cu^{+} by SO_2 for SCR of NO over Fe-Cu/TiO_2-CNTs catalysts, and the Cu^{+} ions were active components at high temperatures. Here in this study, we found that for CuO-CeO_2, CeO_2 suppressed the Cu^{2+} reduction which could be attributed to the redox cycle between Ce^{4+} and Ce^{3+} [12, 16, 17], and thus Cu^{+} was not detected by XPS even after the catalyst was tested with SO_2. As a result, the CuO-CeO_2 showed the potential to keep high NO removal activity even with SO_2.

The S 2p bands of $SD_{[1\%]}(90)$, $SD_{[5\%]}(300)$, and $SD_{[10\%]}(540)$ samples were showed in Fig. 5d. The binding energy of S 2p concentrated at about 168.2-168.5 eV and 169.2-169.7 eV corresponded to S^{4+} and S^{6+}, respectively [35, 37]. It is also worth noting that, the surface atomic concentration of S was 1.34% over $SD_{[1\%]}(90)$, which indicated that deposition of ammonia sulfate/sulfites at the catalyst surface occurred during NO reduction with SO_2 [6, 8, 21]. And a surface S concentration of 1.34% is sufficient to deactivate the catalyst. Interestingly, on the one hand, the deposited S species on catalyst surface increased to 3.13% over $SD_{[5\%]}(300)$; on the other hand, the SO_2 induced catalyst deactivation weakened as shown in Fig. 2. This strongly suggested that the deactivation caused by sulfate/sulfites deposition could be minimized by increasing the O_2 concentration. Moreover, in the case of high O_2 concentration of 10.0 vol%, sulfate/sulfites deposition was also suppressed and the surface S concentration reduced to 1.68% over $SD_{[10\%]}(540)$, which should further suppress the SO_2 induced deactivation.

From Fig. 5d, the ratio of $S^{4+}/(S^{4+}+ S^{6+})$ over $SD_{[1\%]}(90)$, $SD_{[5\%]}(300)$, and $SD_{[10\%]}(540)$ was calculated to be 30.7%, 41.9%, and 60.6%, respectively. Normally, sulfites are ready to be oxidized to sulfates by O_2. However, the ratio of $S^{4+}/(S^{4+}+ S^{6+})$ decreased with O_2 concentration, which suggested the existence of an additional reaction to reduce S^{6+} to S^{4+}.

4. Discussions

The deactivation of catalyst by SO_2 at low temperature is the main barrier for the application of low temperature SCR of NO [6, 8, 20-23], which was mainly due to the deposition of ammonia sulfate/sulfites. Over $CuO-CeO_2$ in this study, SO_2 also induced deposition of ammonia sulfate/sulfite and catalyst deactivation under 1.0 vol% O_2 as shown in Figs. 2 and 5d at 240 °C. Amazingly, under O_2 concentration above 5.0 vol% (especially 10.0 vol%), the SO_2 induced deactivation was weakened, though surface sulfate/sulfite deposition still occurred. From literature, introducing NO_2 into the reaction system, together with the adding of CeO_2 into the catalysts, was found to promote the tolerance SO_2 deactivation [24, 25, 30, 38]. Therefore it seems high concentration of O_2 and Ce species (in catalyst) could restrain the deactivation of catalyst by SO_2; accordingly, the related reactions involved in this system were analyzed and listed as below:

$$8NO + 8NH_3 + O_2 + 4CuO\text{-}4CeO_2 \rightarrow 8N_2 + 12H_2O + 2Cu_2O\text{-}4CeO_2 \qquad (1)$$

$$2NO + O_2 \rightarrow 2NO_2 \qquad (2)$$

$$NO + 2CuO\text{-}2CeO_2 \rightarrow NO_2 + Cu_2O\text{-}2CeO_2 \qquad (3)$$

$$NO + NO_2 + 2NH_3 \rightarrow 2N_2 + 3H_2O \qquad (4)$$

$$6NO_2 + 8NH_3 \rightarrow 7N_2 + 12H_2O \qquad (5)$$

$$SO_2 + 2NH_3 + H_2O \rightarrow (NH_4)_2SO_3 \qquad (6)$$

$$2(NH_4)_2SO_3 + O_2 \rightarrow 2(NH_4)_2SO_4 \qquad (7)$$

$$Cu_2O\text{-}2CeO_2 \rightarrow 2CuO + Ce_2O_3 \qquad (8)$$

$$Cu_2O\text{-}Ce_2O_3 + O_2 \rightarrow 2CuO\text{-}2CeO_2 \qquad (9)$$

$$4(NH_4)_2SO_4 + 2(4\text{-}x)NO_2 \rightarrow (4\text{-}x)N_2 + 4(NH_{X<3})_2SO_4 + 4(4\text{-}x)H_2O \qquad (10)$$

$$(NH_{X<3})_2SO_4 + (2\text{-}x)Ce_2O_3 \rightarrow N_2 + SO_2 + xH_2O + 2(2\text{-}x)CeO_2 \qquad (11)$$

Reaction (1) is the standard SCR reaction normally occurred at high temperatures, by which the lattice oxygen in the catalyst was also involved. Reactions (2) and (3) produced sufficient NO_2 which promoted the SCR reaction through the fast reaction (4) and/or reactions (5) + (10) at low temperatures. At the same time SO_2 was also involved in reactions (6) and (7), which was proved by XPS as shown in Fig. 5d. The produced Cu_2O (normally only part of Cu^{2+} ions were reduced, here for simplification, we direct use Cu_2O as formulas of Cu_XO containing Cu^+. Similarly, Ce_2O_3 was used as formulas of Ce_XO containing Ce^{3+}) from reactions (1) and (3) was then oxidized by CeO_2 through reaction (8); as a result, Cu^+ was not detected as shown in Fig. 5c. The reduced catalyst could also be oxidized by O_2 through reaction (9). In fact, reactions (9) and (11) explained the low Ce^{3+} ions detected over catalyst

$SD_{[10\%]}(540)$ as shown in Fig. 5b. Compared to reaction (5), reaction (10) is also reasonable, which also produced $NH_{X<3}$ species with high oxidability, thus reduced the surface S^{6+} concentration through reaction (11), especially under 10.0 vol% of O_2, which produced sufficient NO_2 through reactions (2) and (3). Note that from the free Gibbs energy calculation, reduction of S^{6+} to S^{4+} through reaction (11) is energetically favored. As a result, the catalyst deactivation caused by sulfate deposition could be weakened or even minimized through reactions (8), (10) and (11). Here the direct oxidation of SO_2 to SO_3 was neglected because the low reaction temperature (below 240 °C). The fact that Cu^+ was not detected by XPS from catalysts after SO_2 induced deactivation, together with the decrease of surface S concentration and increase of surface S^{4+} species as shown in Fig. 5, strongly supported our proposal. From Fig. 2, the catalyst regeneration under 10 vol% O_2 with NH_3 and NO only (in section E) was also shown, evidently the atmosphere with NH_3 + NO + O_2 showed the best effect for catalyst recovery, which strongly suggested that NH_3 + NO + O_2 produced new deoxidizer of $NH_{X<3}$ to promote the reaction for S^{6+} to S^{4+}. Since NO_2 is a strong oxidizer compared to NO, the production of deoxidizer like $NH_{X<3}$ as intermediate product is very reasonable [1], from the reactants involved in the above reactions, $NH_{X<3}$ is the only deoxidizer possibly produced.

In order to further confirm our proposal, TGA curves were used to analysis the thermal stability of fresh catalyst and $SD_{[10\%]}(540)$. As shown in Fig. 6, the TG curve of fresh catalyst almost showed no weight loss up to 600 °C. While for the TG curve of $SD_{[10\%]}(540)$, a weight loss of approximately 5% and 2% was observed at 200-300 °C and 300-400 °C, which could be corresponded to the decomposition of ammonia sulfate and sulfite, respectively [39]. This is in good agreement with the calculated ratio of $S^{4+}/(S^{4+}+S^{6+})$ from $SD_{[10\%]}(540)$.

FTIR was also used to characterize the $CuO\text{-}CeO_2$ catalyst at different reaction stages. As shown in Fig. 7, peaks located at 1384 cm^{-1} and 1623 cm^{-1} attributed to the surface NO_2^- (monodentate nitrito) and NO_3^- (bidentate) were detected in all spectra, indicating the success adsorption of NO and NO_2, and a strong intensity of peak at 1623 cm^{-1} (compared to the intensity of peak 1384 cm^{-1}) was observed in spectra –c and –e under reaction with SO_2 [40-42], indicating that surface NO_2 species increased with SO_2 introduction, which should be beneficial for NO removal. Also, peaks at 1050 cm^{-1} (attributed to SO_4^{2-}) and at 976 and 1150 (attributed SO_3^{2-}) were detected in spectra –c and –e [33, 43-47], indicating the deposition of sulfate/sulfite, in agreement with our XPS measurements. Note that the intensity of SO_3^{2-} peaks in spectrum-e was stronger than those in spectrum-c, which strongly supported our assumption of the existence of sulfate decomposition at low temperature as reactions -10 and -11 shown. By the way, a weak peak at 1050 cm^{-1} could also be observed in spectra –a, –b , and –d, which could be caused by the trace SO_2 remained in the test system, the peaks located at 844 cm^{-1} was attributed to the surface Cu^{2+} [47], however, the attribution of peak at 780 cm^{-1} is still not clear.

5 Conclusions

In summary, CuO-CeO_2 catalyst deactivation caused by the deposition of ammonia sulfate/sulfite could be online reactivated with 5.0 vol% O_2 at 240 °C, which was attributed to the reaction between NH_3/NH_4^+ and NO_2. Under 10.0 vol% O_2, the SO_2 deactivation was minimized, and the reaction between $Ce_2O_3 + NH_{X<3}$ and ammonia sulfates overcame the accumulation of sulfate on the catalyst surface. The results obtained in this study provided a possibility to suppress the SO_2 induced catalyst deactivation at low temperatures, which should be important for the applications of low temperature SCR.

Acknowledgments: This work was supported by the Environmentally Sustainable Management of Medical Wastes in China (Contract No. C/V/S/10/251), the National Natural Foundation of Zhejiang Province, China (Grant No.Z4080070), and Zhejiang Province Environmental Protection Science Research Plan of China (2011B14).

References:

1. Qi, G. S.; Yang, R. T.; Chang, R., MnO_X-CeO_2 mixed oxides prepared by co-precipitation for selective catalytic reduction of NO with NH_3 at low temperatures. *Applied Catalysis B: Environmental* **2004,** 51, (2), 93-106.

2. Eigenmann, F.; Maciejewski, M.; Baiker, A., Selective reduction of NO by NH_3 over manganese-cerium mixed oxides: Relation between adsorption, redox and catalytic behavior. *Applied Catalysis B: Environmental* **2006,** 62, (3-4), 311-318.

3. Long, R. Q.; Yang, R. T., Catalytic performance of Fe-ZSM-5 catalysts for selective catalytic reduction of nitric oxide by ammonia. *Journal of Catalysis* **1999,** 188, (2), 332-339.

4. Long, R. Q.; Yang, R. T., Superior Fe-ZSM-5 catalyst for selective catalytic reduction of nitric oxide by ammonia. *Journal of the American Chemical Society* **1999,** 121, (23), 5595-5596.

5. Kroecher, O.; Elsener, M., Combination of V_2O_5/WO_3-TiO_2, Fe-ZSM-5, and Cu-ZSM-5 Catalysts for the Selective Catalytic Reduction of Nitric Oxide with Ammonia. *Industrial & Engineering Chemistry Research* **2008,** 47, (22), 8588-8593.

6. Ma, Z.; Yang, H.; Liu, F.; Zhang, X., Interaction between SO_2 and Fe-Cu-O_X/CNTs-TiO_2 catalyst and its influence on NO reduction with NH_3. *Applied Catalysis A: General* **2013,** 467, 450-455.

7. Ma, Z.; Yang, H.; Li, Q.; Zheng, J.; Zhang, X., Catalytic reduction of NO by NH_3 over Fe-Cu-O-$_X$/CNTs-TiO_2 composites at low temperature. *Applied*

Catalysis A: General **2012,** 427, 43-48.

8. Ma, Z.; Yang, H.; Li, B.; Liu, F.; Zhang, X., Temperature-Dependent Effects of SO_2 on Selective Catalytic Reduction of NO over Fe-Cu-O_X/CNTs-TiO_2 Catalysts. *Industrial & Engineering Chemistry Research* **2013,** 52, 3708-3713.

9. Li, Q.; Yang, H.; Nie, A.; Fan, X.; Zhang, X., Catalytic Reduction of NO with NH_3 over V_2O_5-MnO_X/TiO_2-Carbon Nanotube Composites. *Catalysis Letters* **2011,** 141, (8), 1237-1242.

10. Li, Q.; Hou, X.; Yang, H.; Ma, Z.; Zheng, J.; Liu, F.; Zhang, X.; Yuan, Z., Promotional effect of CeO_X for NO reduction over V_2O_5/TiO_2-carbon nanotube composites. *Journal of Molecular Catalysis A: Chemical* **2012,** 356, 121-127.

11. Fan, X.; Qiu, F.; Yang, H.; Tian, W.; Hou, T.; Zhang, X., Selective catalytic reduction of NO_X with ammonia over Mn-Ce-O_X/TiO_2-carbon nanotube composites. *Catalysis Communications* **2011,** 12, (14), 1298-1301.

12. Bera, P.; Priolkar, K. R.; Sarode, P. R.; Hegde, M. S.; Emura, S.; Kumashiro, R.; Lalla, N. P., Structural investigation of combustion synthesized Cu/CeO_2 catalysts by EXAFS and other physical techniques: Formation of a $Ce_{1-X}Cu_XO_2$-delta solid solution. *Chemistry of Materials* **2002,** 14, (8), 3591-3601.

13. Chen, L.; Li, J.; Ge, M., Promotional Effect of Ce-doped V_2O_5-WO_3/TiO_2 with Low Vanadium Loadings for Selective Catalytic Reduction of NO_X by NH_3. *Journal of Physical Chemistry C* **2009,** 113, (50), 21177-21184.

14. Liu, Z. L.; Fu, Y. L.; Tu, J.; Meng, M., Effect of CeO_2 on supported Pd

catalyst in the SCR of NO: A DRIFT study. *Catalysis Letters* **2002,** 81, (3-4), 285-291.

15. Reddy, B. M.; Khan, A.; Yamada, Y.; Kobayashi, T.; Loridant, S.; Volta, J. C., Structural characterization of CeO_2-TiO_2 and V_2O_5/CeO_2-TiO_2 catalysts by Raman and XPS techniques. *Journal of Physical Chemistry B* **2003,** 107, (22), 5162-5167.

16. Chen, J.; Zhu, J.; Zhan, Y.; Lin, X.; Cai, G.; Wei, K.; Zheng, Q., Characterization and catalytic performance of Cu/CeO_2 and Cu/MgO-CeO_2 catalysts for NO reduction by CO. *Applied Catalysis A: General* **2009,** 363, (1-2), 208-215.

17. Wu, X.; Liang, Q.; Weng, D.; Lu, Z., The catalytic activity of CuO-CeO_2 mixed oxides for diesel soot oxidation with a NO/O_2 mixture. *Catalysis Communications* **2007,** 8, (12), 2110-2114.

18. Gao, X.; Du, X.; Cui, L.; Fu, Y.; Luo, Z.; Cen, K., A Ce-Cu-Ti oxide catalyst for the selective catalytic reduction of NO with NH_3, *Catalysis Communications* **2010,**12, 255-258.

19. Pan, W.; Zhou, Y.; Guo, R.; Zhen, W.; Hong, J.; Xu, H.; Jin, Q.; Ding, C.; Guo, S., Influence of calcination temperature on CeO_2-CuO catalyst for the selective catalytic reduction of NO with NH_3, *Environmental Progress & Sustainable Energy* **2014,** 33, 385-389.

20. Xu, W.; He, H.; Yu, Y., Deactivation of a Ce/TiO_2 Catalyst by SO_2 in the Selective Catalytic Reduction of NO by NH_3. *Joural of Physical Chemistry C*

2009, 113, (11), 4426-4432.

21. Xie, G. Y.; Liu, Z. Y.; Zhu, Z. P.; Liu, Q. Y.; Ge, J.; Huang, Z. G., Simultaneous removal of SO_2 and NO_X from flue gas using a CuO/Al_2O_3 catalyst sorbent I. Deactivation of SCR activity by SO_2 at low temperatures. *Journal of Catalysis* **2004,** 224, (1), 36-41.

22. Jin, R.; Liu, Y.; Wu, Z.; Wang, H.; Gu, T., Relationship between SO_2 poisoning effects and reaction temperature for selective catalytic reduction of NO over Mn-Ce/TiO_2 catalyst. *Catalysis Today* **2010,** 153, (3-4), 84-89.

23. Du, X.; Gao, X.; Cui, L.; Fu, Y.; Luo, Z.; Cen, K., Investigation of the effect of Cu addition on the SO_2 resistance of a CeTi oxide catalyst for selective catalytic reduction of NO with NH_3. *Fuel* **2012,** 92, (1), 49-55.

24. Wijayanti, K.; Andonova, S.; Kumar, A.; Li, J. H.; Kamasamudram, K.; Currier, N. W.; Yezerets, A.; Olsson, L., Impact of sulfur oxide on NH_3-SCR over Cu-SAPO-34, *Applied Catalysis B: Environmental* **2015**, 166-167, 568-579.

25. Colombo, M.; Nova, I.; Tronconi, E., Detailed kinetic modeling of the NH_3–NO/NO_2 SCR reactions over a commercial Cu-zeolite catalyst for diesel exhausts after treatment, *Catalysis Today* **2012**, 197, 243-255.

26. Pinaeva, L. G.; Sadovskaya, E. M.; Suknev, A. P.; Goncharov, V. B.; Sadykov, V. A.; Balzhinimaev, B. S.; Decamp, T.; Mirodatos, C., On the oxygen effect in nitric oxide reduction by methane over Co/ZSM-5. *Chemical Engineering Science* **1999,** 54, (20), 4327-4335.

27. Jiang, B.; Li, Z.; Lee, S., Mechanism study of the promotional effect of O_2 on low-temperature SCR reaction on Fe-Mn/TiO_2 by DRIFT. *Chemical Engineering Journal* **2013,** 225, 52-58.

28. Djerad, S.; Crocoll, M.; Kureti, S.; Tifouti, L.; Weisweiler, W., Effect of oxygen concentration on the NOx reduction with ammonia over V_2O_5-WO_3/TiO_2 catalyst. *Catalysis Today* **2006,** 113, (3-4), 208-214.

29. Chi, Y.; Chuang, S., The effect of oxygen concentration on the reduction of NO with propylene over CuO/gamma-Al_2O_3. *Catalysis Today* **2000,** 62, (4), 303-318.

30. Wang, Y. L.; Li, X. X.; Zhan, L.; Li, C.; Qiao, W. M.; Ling, L. C., Effect of SO_2 on activated carbon honeycomb supported CeO_2-MnO_X catalyst for NO removal at low temperature, *Industrial & Engineering Chemistry Research* **2015,** 54, 2274-2278.

31. Koebel, M.; Madia, G.; Elsener, M., Selective catalytic reduction of NO and NO_2 at low temperatures. *Catalysis Today* **2002,** 73, (PII S0920-5861(02)00006-83-4), 239-247.

32. Liu, F.; Asakura, K.; He, H.; Shan, W.; Shi, X.; Zhang, C., Influence of sulfation on iron titanate catalyst for the selective catalytic reduction of NO_X with NH_3. *Applied Catalysis B: Environmental* **2011,** 103, (3-4), 369-377.

33. Wang, J.; Zhu, Z.; Li, C., Pathway of the cycle between the oxidative adsorption of SO_2 and the reductive decomposition of sulfate on the $MgAl_{2-X}Fe_XO_4$

catalyst. *Journal of Molecular Catalysis A: Chemical* **1999,** (139), 31-41.

34. Holgado, J. P.; Alvarez, R.; Munuera, G., Study of CeO_2 XPS spectra by factor analysis: reduction of CeO_2. *Applied Surface Science* **2000,** 161, (3-4), 301-315.

35. Smirnov, M. Y.; Kalinkin, A. V.; Pashis, A. V.; Sorokin, A. M.; Noskov, A. S.; Kharas, K. C.; Bukhtiyarov, V. I., Interaction of Al_2O_3 and CeO_2 surfaces with SO_2 and SO_2+O_2 studied by X-ray photoelectron spectroscopy. *Journal of Physical Chemistry B* **2005,** 109, (23), 11712-11719.

36. Poulston, S.; Parlett, P. M.; Stone, P.; Bowker, M., Surface oxidation and reduction of CuO and Cu_2O studied using XPS and XAES. *Surface and Interface Analysis* **1996,** 24, (12), 811-820.

37. Romano, E. J.; Schulz, K. H., A XPS investigation of SO_2 adsorption on ceria-zirconia mixed-metal oxides. *Applied Surface Science* **2005,** 246, (1-3), 262-270.

38. Huang, Z.; Zhu, Z.; Liu, Z.; Liu, Q., Formation and reaction of ammonium sulfate salts on V_2O_5/AC catalyst during selective catalytic reduction of nitric oxide by ammonia at low temperatures. *Journal of Catalysis* **2003,** 214, (2), 213-219.

39. Yu, J.; Guo, F.; Wang, Y.; Zhu, J.; Liu, Y.; Su, F.; Gao, S.; Xu, G., Sulfur poisoning resistant mesoporous Mn-base catalyst for low-temperature SCR of NO with NH_3. *Applied Catalysis B: Environmental* **2010,** 95, (1-2), 160-168.

[40] Kantcheva, M., FT-IR spectroscopic investigation of the reactivity of NO_X species adsorbed on Cu^{2+}/ZrO_2 and $CuSO_4/ZrO_2$ catalysts toward decane. *Applied Catalysis B: Environmental* **2003,** 42, 89-109.

[41] Yamazoe, S.; Okumura, T.; Hitomi, Y.; Shishido, T.; Tanaka, T., Mechanism of photo-oxidation of NH_3 over TiO_2: Fourier transform infrared study of the intermediate species. *Journal of Physical Chemistry C* **2007,** 111, 11077-11085.

[42] Chen, Y.; Wang, J.; Yan, Z.; Liu, L.; Zhang, Z.; Wang, X., Promoting effect of Nd on the reduction of NO with NH_3 over CeO_2 supported by activated semi-coke: an in situ DRIFTS study, *Catalysis Science & Technololgy* **2015,** 5, 2251-2259.

[43] Lee, Y.; Park, J.; Choung, J.; Choi, D., Adsorption characteristics of SO_2 on activated carbon prepared from coconut shell with potassium hydroxide activation, *Environmental Science & Technology* **2002,** 36, 1086-1092.

[44] Quijada, C.; Rodes, A.; Vazquez, J.; Perez, J.; Aldaz, A., Electrochemical behaviour of aqueous SO_2 at Pt electrodes in acidic medium. A voltammetric and in situ Fourier transform IR study Part I. Oxidation of SO_2 on Pt electrodes with sulphur-oxygen adsorbed species, *Journal of Electroanalytical Chemistry* **1995,** 394, 217-227.

[45] Datta, A.; Cavell, R. G., Claus Catalysis. 1. Adsorption of SO_2 on the alumina catalyst studied by FTIR and EPR spectroscopy, *Journal of Physical Chemistry* **1985,** 89, 443-449.

[46] Degenhardt, J.; McQuillan, A. J., In situ ATR-FTIR spectroscopic study of adsorption of perchlorate, sulfate, and thiosulfate ions onto chromium(III) oxide hydroxide thin films, *Langmuir* **1999,** 15, 4595-4602.

[47] Shen, M.; Wen, H.; Hao, T.; Yu, T.; Fan, D.; Wang, J.; Li, W.; Wang, J., Deactivation mechanism of SO_2 on Cu/SAPO-34 NH_3-SCR catalysts: Structure and active Cu^{2+}, *Catalysis Science & Technology* **2015,** 5, 1741-1749.

Figure Captions:

Fig.1. NO conversion over CuO-CeO_2, under 550 ppm of NO +550 ppm NH_3+ 1-10 vol % O_2 + Ar, at a total flow rate of 500 ml/min and a gas hourly space velocity (GHSV) of 150,000 h^{-1} at 160, 180, 200, 220, and 240 °C.

Fig.2. Effects of O_2 on SO_2 deactivation and regeneration at 240 °C. Section-A: activity characterization of the fresh catalyst with 1 vol% O_2; section-B: deactivation by introducing 200 ppm SO_2; section-C: regeneration with 550 ppm NO, 550 ppm NH_3, 5 vol% O_2, and Ar balance; section-D: deactivation again with 200 ppm SO_2 introducing; section-E: regeneration again with 550 ppm NO, 550 ppm NH_3, 10 vol% O_2, and Ar balance; and section-F: catalyst deactivation with 200 ppm SO_2. For comparison, the activity of catalyst after regeneration with 550 ppm NO + 10.0 vol% and 550 ppm NH_3 + 10.0 vol% in section -E was also shown in section-F (blue and red line, respectively).

Fig.3. NO oxidation under 550 ppm of NO + 1-10 vol % O_2 + Ar, at a total flow rate of 500 ml/min and a gas hourly space velocity (GHSV) of 150,000 h^{-1}.

Fig.4. (a) NH_3-TPD pattern; and (b) NH_3-TPO profiles of the catalyst.

Fig.5. XPS results of (a) O 1s, (b) Ce 3d, (c) Cu 2p, and (d)S 2p for (i) CuO-CeO_2, (ii) $SD_{[1\%]}$(90), (iii) $SD_{[5\%]}$(300), and (iv) $SD_{[10\%]}$(540), respectively.

Fig.6. TG analysis at 10 °C/min for fresh catalyst and $SD_{[10\%]}$(540).

Fig. 7. FTIR spectra of CuO-CeO_2 after 12 hours treatment at 240°C for (a) N_2 purging; (b) SCR test under 800 ppm NO, 800 ppm NH_3 and 5% O_2; (c) SCR test

---

under 800 ppm NO, 800 ppm NH_3, 200ppm SO_2 and 5% O_2; (d) SCR test under 800 ppm NO, 800 ppm NH_3 and 10% O_2; and (e) SCR test under 800 ppm NO, 800 ppm NH_3, 200ppm SO_2 and 10% O_2.

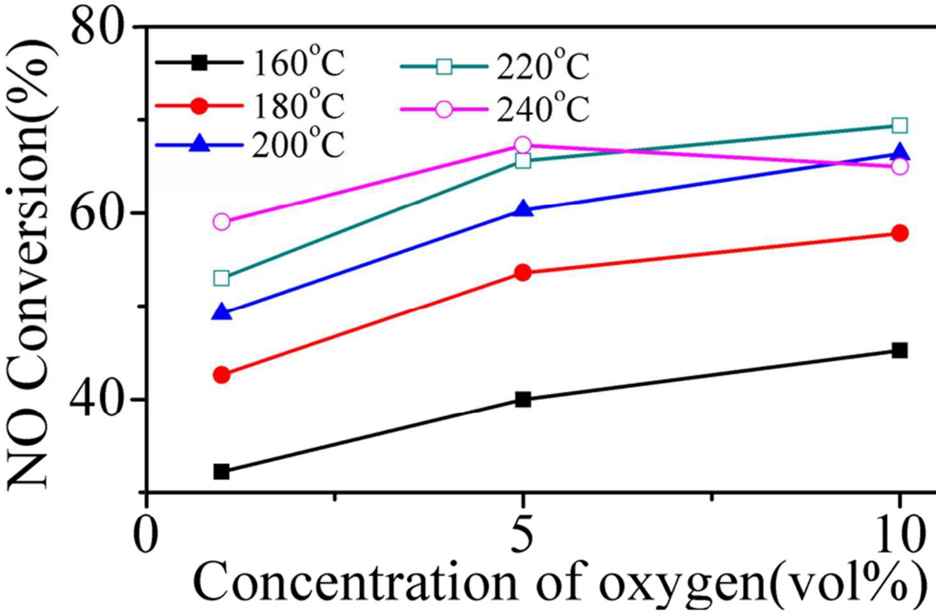

Fig.1. NO conversion over CuO-CeO2, under 550 ppm of NO +550 ppm NH3+ 1-10 vol % O2 + Ar, at a total flow rate of 500 ml/min and a gas hourly space velocity (GHSV) of 150,000 h-1 at 160, 180, 200, 220, and 240 °C.
80x49mm (300 x 300 DPI)

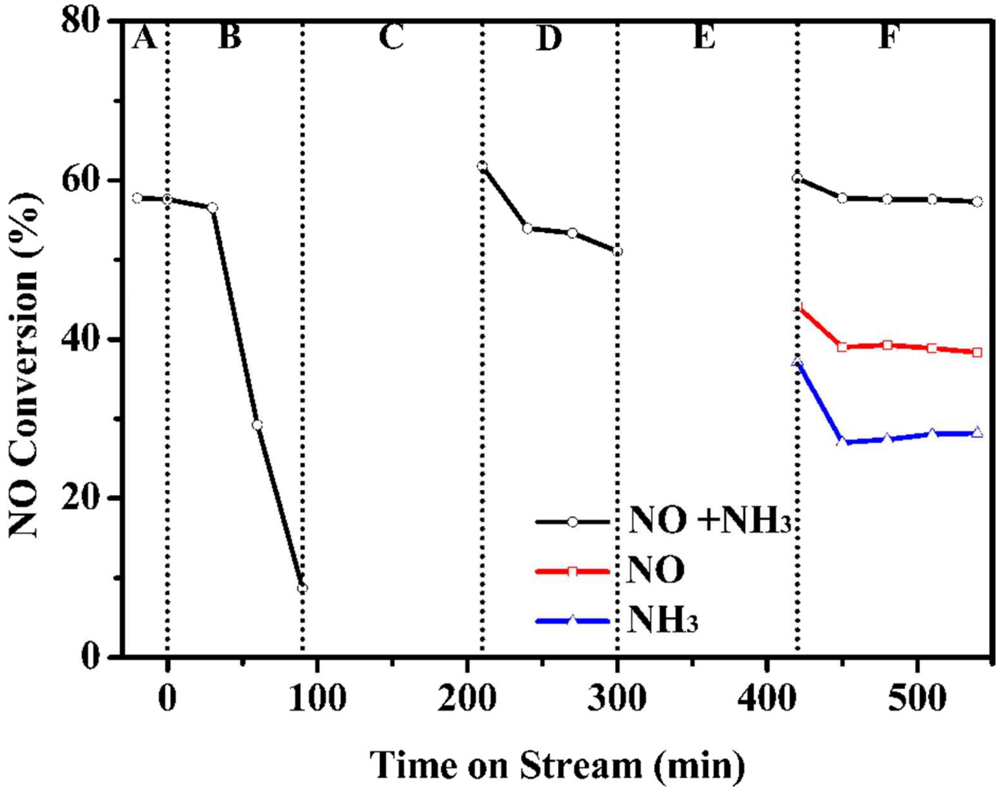

Fig.2. Effects of O2 on SO2 deactivation and regeneration at 240 °C. Section-A: activity characterization of the fresh catalyst with 1 vol% O2; section-B: deactivation by introducing 200 ppm SO2; section-C: regeneration with 550 ppm NO, 550 ppm NH3, 5 vol% O2, and Ar balance; section-D: deactivation again with 200 ppm SO2 introducing; section-E: regeneration again with 550 ppm NO, 550 ppm NH3, 10 vol% O2, and Ar balance; and section-F: catalyst deactivation with 200 ppm SO2. For comparison, the activity of catalyst after regeneration with 550 ppm NO + 10.0 vol% and 550 ppm NH3 + 10.0 vol% in section -E was also shown in section-F (blue and red line, respectively).
80x63mm (300 x 300 DPI)

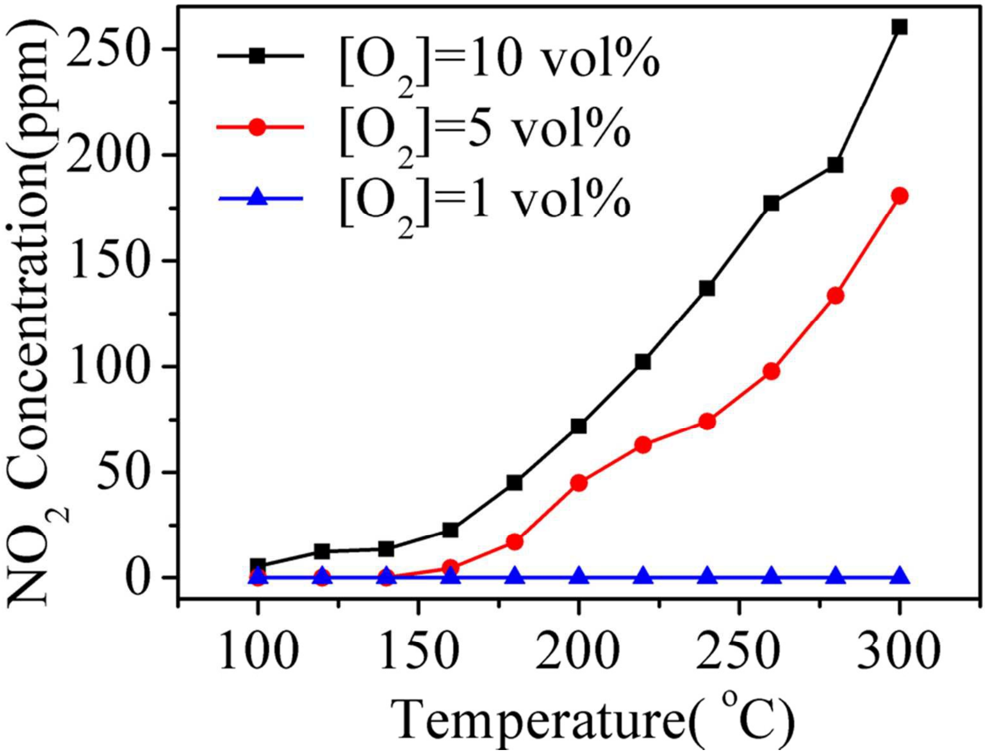

Fig.3. NO oxidation under 550 ppm of NO + 1-10 vol % O2 + Ar, at a total flow rate of 500 ml/min and a gas hourly space velocity (GHSV) of 150,000 h-1
80x60mm (300 x 300 DPI)

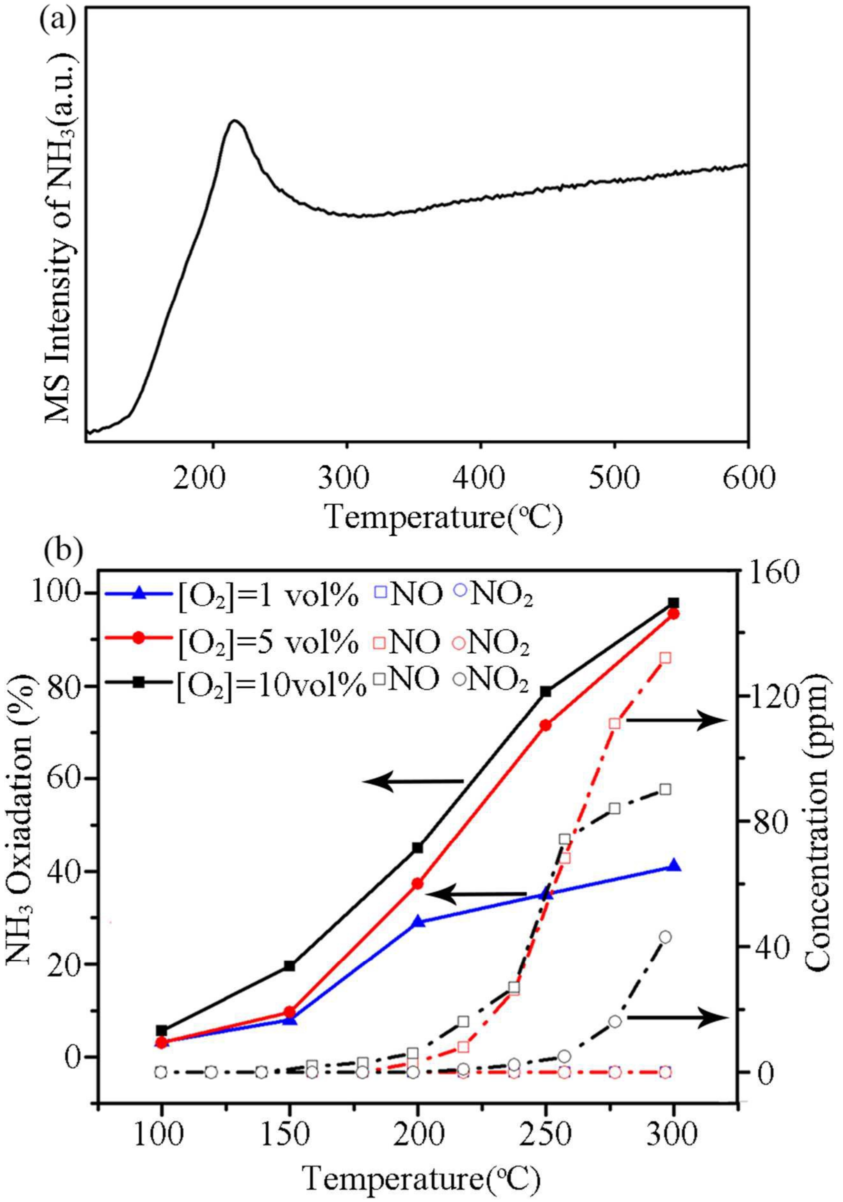

80x114mm (300 x 300 DPI)

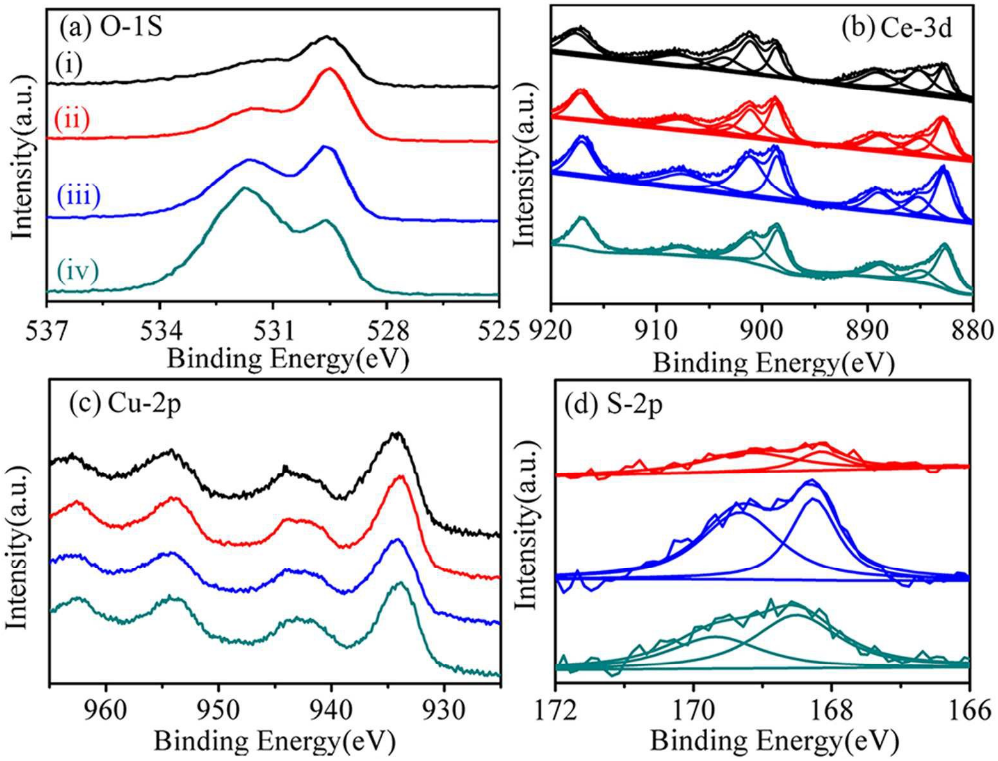

Fig.5. XPS results of (a) O 1s, (b) Ce 3d, (c) Cu 2p, and (d)S 2p for (i) CuO-CeO2, (ii) SD[1%](90), (iii) SD[5%](300), and (iv) SD[10%](540), respectively.
85x65mm (300 x 300 DPI)

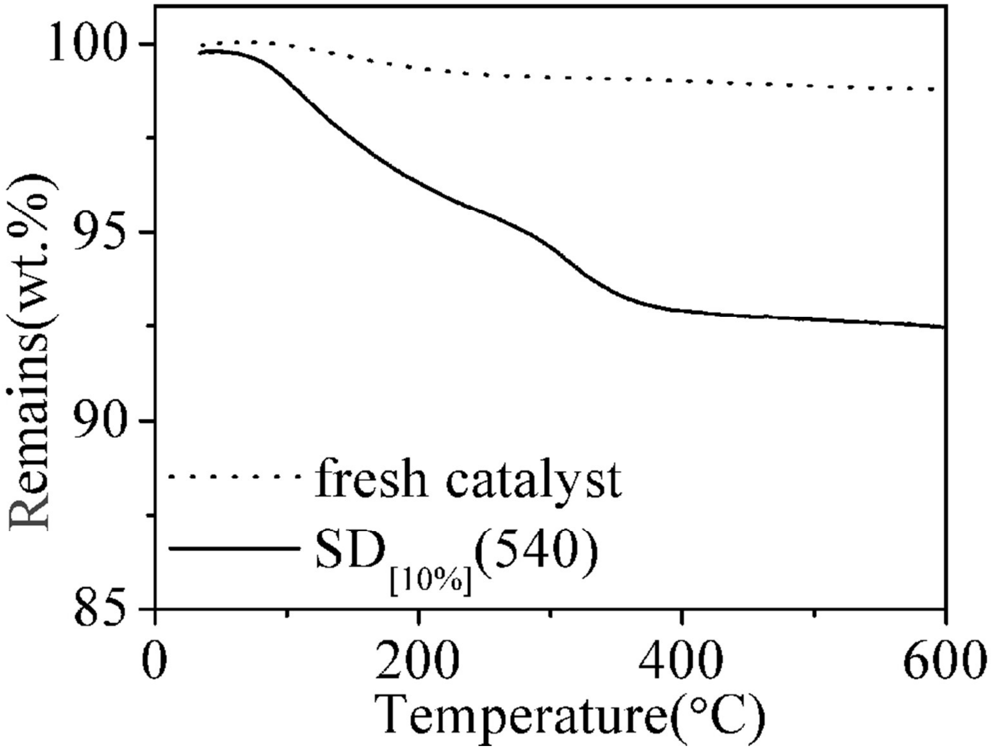

Fig.6. TG analysis at 10 °C/min for fresh catalyst and SD[10%](540)
85x63mm (300 x 300 DPI)

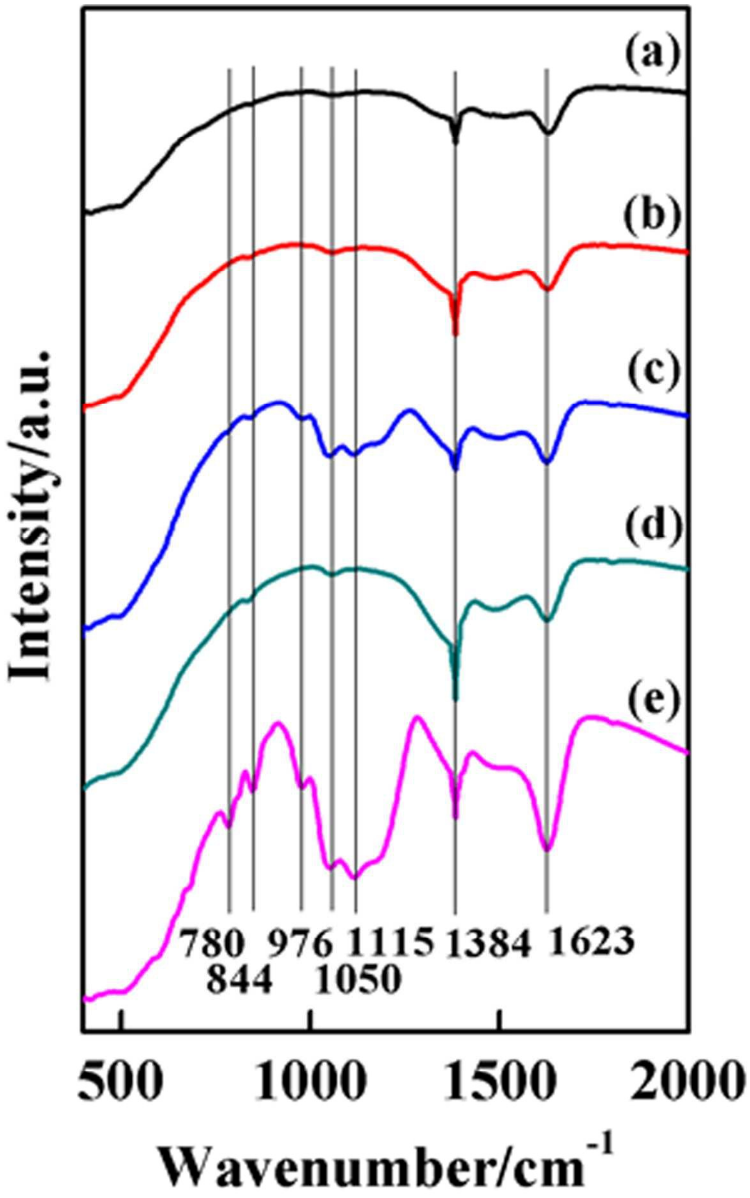

85x127mm (300 x 300 DPI)

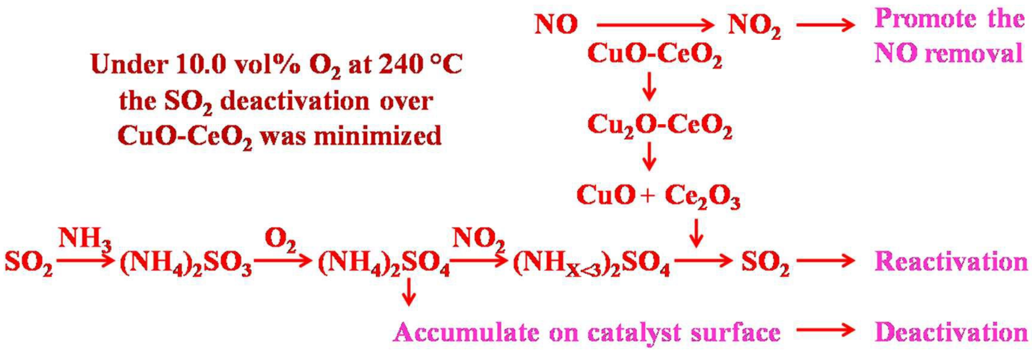

Reaction between NO_2 and NH_3/NH_4^+ induced the formation of $NH_{X<3}$ species with high oxidability; $NH_{X<3}$ promoted the surface sulfate decomposition; high de-NO_X performance was achieved in the presence of SO_2 at low temperature.